PNAS

Supporting Information for
EMT activates exocytotic Rabs to coordinate invasion and immunosuppression in lung cancer

Guan-Yu Xiao, Xiaochao Tan, Bertha L. Rodriguez, Don L. Gibbons, Shike Wang, Chao Wu, Xin Liu, Jiang Yu, Mayra E. Vasquez, Hai T. Tran, Jun Xu, William K. Russell, Cara Haymaker, Younghee Lee, Jianjun Zhang, Luisa Solis, Ignacio I. Wistuba, Jonathan M. Kurie

Guan-Yu Xiao, Jonathan M. Kurie
Email: Guan-Yu.Xiao@uky.edu, JKurie@mdanderson.org

This PDF file includes:

Figures S1 to S8
Tables S1 to S3

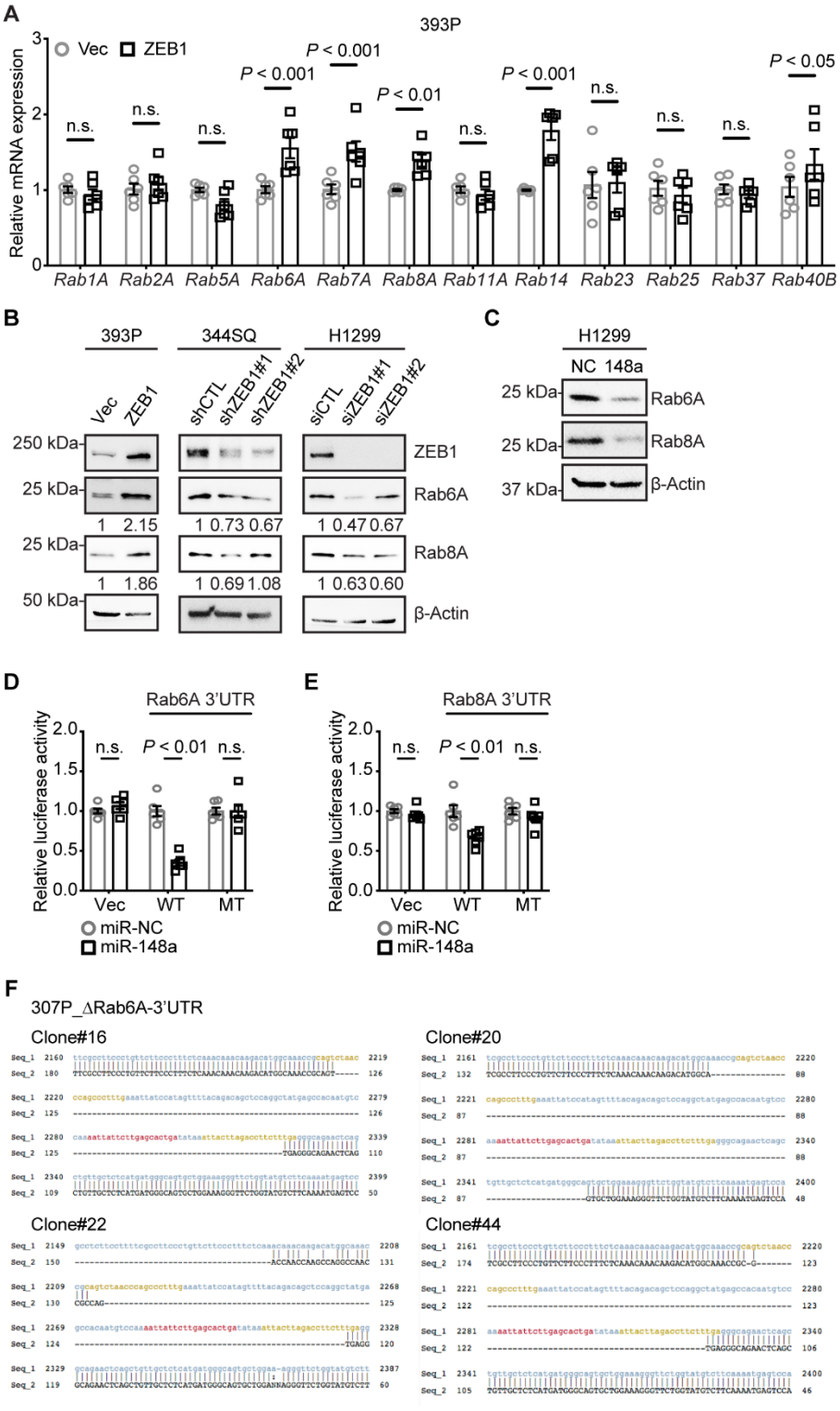
A
393P
Vec
ZEB1
Relative mRNA expression
n.s.
P < 0.001
P < 0.01
P < 0.05
Rab1A
Rab2A
Rab5A
Rab6A
Rab7A
Rab8A
Rab11A
Rab14
Rab23
Rab25
Rab37
Rab40B
B
393P
344SQ
H1299
Vec
ZEB1
shCTL
shZEB1#1
shZEB1#2
siCTL
siZEB1#1
siZEB1#2
250 kDa
25 kDa
50 kDa
ZEB1
Rab6A
Rab8A
β-Actin
1 2.15
1 0.73 0.67
1 0.47 0.67
1 1.86
1 0.69 1.08
1 0.63 0.60
C
H1299
NC
148a
25 kDa
37 kDa
Rab6A
Rab8A
β-Actin
D
Rab6A 3'UTR
Relative luciferase activity
n.s.
P < 0.01
Vec
WT
MT
miR-NC
miR-148a
E
Rab8A 3'UTR
Relative luciferase activity
n.s.
P < 0.01
Vec
WT
MT
miR-NC
miR-148a
F
307P_ΔRab6A-3'UTR
Clone#16
Clone#20
Clone#22
Clone#44

Fig. S1. ZEB1 activates exocytotic Rabs. (A) Q-PCR analysis of Rab family member mRNA levels in 393P_vector cells (Vec) and 393P_ZEB1 cells (ZEB1) (n=6 replicates per condition). (B) Western blot (WB) analysis of Rab6A and Rab8A levels in the indicated transfectants. β-actin loading control. Relative densitometric values indicated. (C) WB analysis of Rab6A and Rab8A in cells transfected with miR-148a mimics or non-coding control (NC). (D, E) Luciferase activities in H1299 cells transiently co-transfected with pre-miR-148a and human Rab6A 3'UTR (D) or Rab8A 3'UTR (E) reporters containing wild-type (WT) or mutant 3'-UTRs lacking predicted miR-148a binding sites (MT). Empty reporters (Vec). Results represent means ± SEM (n= 6 replicates per condition). (F) Alignment of Rab6A 3'UTR sequences (top seq-1) and indicated clone sequences (anti-parallel, bottom seq-2). The sgRNA sequences are in yellow. miR148a binding site is in red.

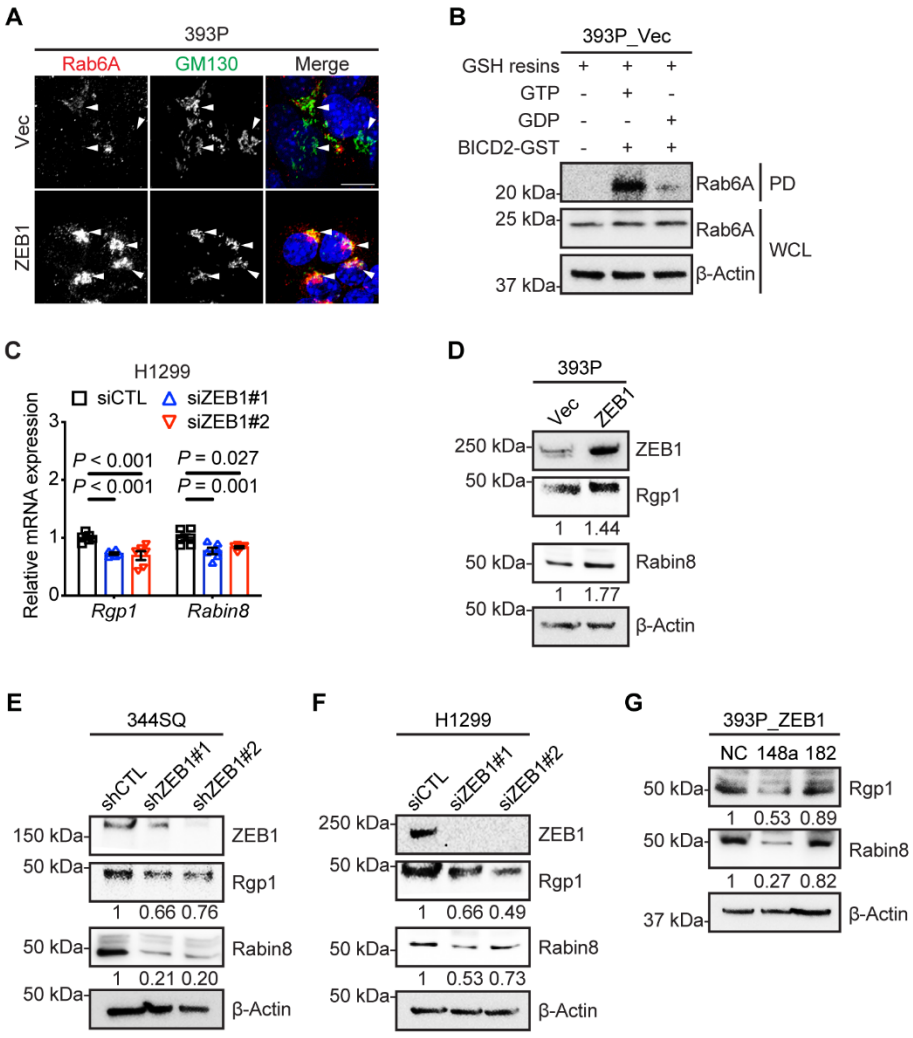

Fig. S2. ZEB1 activates exocytotic Rabs and their GEFs. (A) Confocal micrographs of cells co-stained with anti-Rab6A (red) and -GM130 (green) antibodies. DAPI (blue). Scale bar: 10 μm. (B) Specificity of assays to detect GTP-bound Rab6A in cell lysates. 393P_vector cell lysates were spiked with (200 μM) GTP or GDP and GST-tagged effector protein (BICD2) or GSH resins alone. Lysates were subjected to GST pull-down (PD) and WB analysis was carried out on GST-associated proteins or whole cell lysates (WCL) to detect Rab6A. (C) Q-PCR analysis of Rgp1 and Rabin8 mRNA levels (n=6 replicates per condition). (D-F) WB analysis of Rgp1 and Rabin8 levels in ectopic ZEB1-expressing 393P cells (D), ZEB1-deficient or -replete 344SQ cells (E), and ZEB1-deficient or -replete H1299 cells (F). Empty vector (Vec). β-actin loading control. Relative densitometric values indicated. (G) WB analysis of Rgp1 and Rabin8 levels in miR mimic-transfected 393P_ZEB1 cells. miR-148a (148a). miR-182 (182). non-coding control (NC). Relative densitometric values indicated.

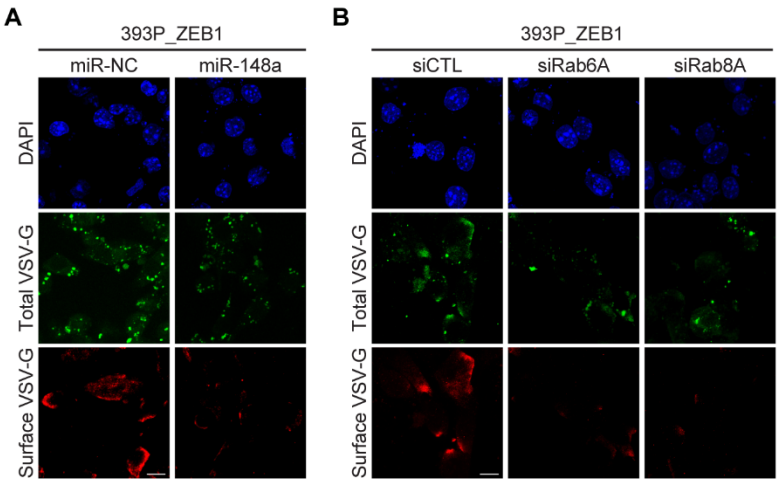

Fig. S3. ZEB1 accelerates exocytotic trafficking by relieving Rab6A and Rab8A from miR-148a-dependent silencing. (A, B) Confocal micrographs of EGFP-tsVSV-G-transfected cells taken 1 h after transfer to permissive temperature. Scale bar, 10 μm.

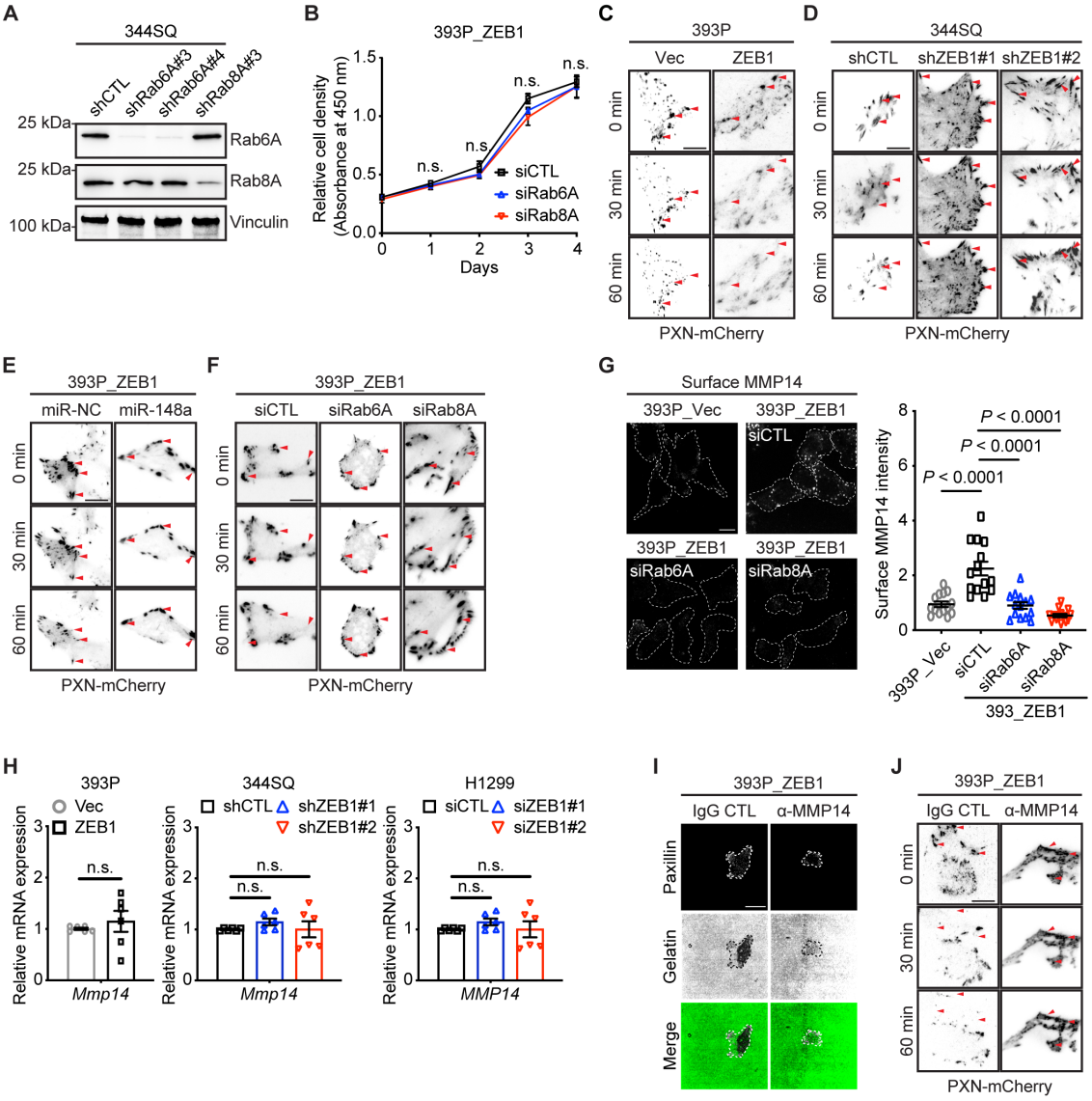
A
344SQ
shCTL
shRab6A#3
shRab6A#4
shRab8A#3
25 kDa
Rab6A
25 kDa
Rab8A
100 kDa
Vinculin
B
393P_ZEB1
Relative cell density (Absorbance at 450 nm)
Days
n.s.
siCTL
siRab6A
siRab8A
C
393P
Vec
ZEB1
0 min
30 min
60 min
PXN-mCherry
D
344SQ
shCTL
shZEB1#1
shZEB1#2
PXN-mCherry
E
393P_ZEB1
miR-NC
miR-148a
PXN-mCherry
F
393P_ZEB1
siCTL
siRab6A
siRab8A
PXN-mCherry
G
Surface MMP14
393P_Vec
393P_ZEB1
siCTL
siRab6A
siRab8A
Surface MMP14 intensity
P < 0.0001
393_ZEB1
H
393P
344SQ
H1299
Vec
ZEB1
shCTL
shZEB1#1
shZEB1#2
siCTL
siZEB1#1
siZEB1#2
Relative mRNA expression
Mmp14
MMP14
I
393P_ZEB1
IgG CTL
α-MMP14
Paxillin
Gelatin
Merge
J
393P_ZEB1
IgG CTL
α-MMP14
PXN-mCherry

Fig. S4. ZEB1 accelerates FA disassembly by relieving Rab6A and Rab8A from miR-148a-dependent silencing. (A) WB analysis of Rab6A and Rab8A levels in 344SQ cells transfected with control (shCTL), Rab6A (shRab6A) or Rab8A (shRab8A) shRNAs. Vinculin loading control. (B) Relative cell density in monolayer culture (n = 8 samples per condition). *P* values were determined using 2-tailed Student's t test. (C-F) Representative TIRF micrographs of KP cells subjected to ectopic ZEB1 expression (C), shRNA-mediated ZEB1 depletion (D), ectopic miR-148a expression (E), or siRNA-mediated Rab6A or Rab8A depletion (F). Disassembling FAs detected by paxillin–mCherry (arrowheads). Scale bars, 10 μm. (G) Confocal micrographs of non-permeabilized cells stained with α-MMP14 antibody to detect surface MMP14. Scale bar: 10 μm. Fluorescence values per cell (dot) normalized to 393P_Vec (scatter plot). (H) Q-PCR analysis of *MMP14* mRNA levels in the indicated cells (n=6 replicates per condition). Control shRNA or siRNA sequences (CTL). (I) Confocal micrographs of cells seeded on Oregon Green-488–gelatin, treated for 16 h with IgG or anti-MMP14 neutralizing antibody, and imaged 90 min later. (J) Representative TIRF micrographs of paxillin–mCherry-transfected cells, treated for 16 h with IgG or anti-MMP14 neutralizing antibody. Disassembling FAs (arrowheads). Scale bars, 10 μm.

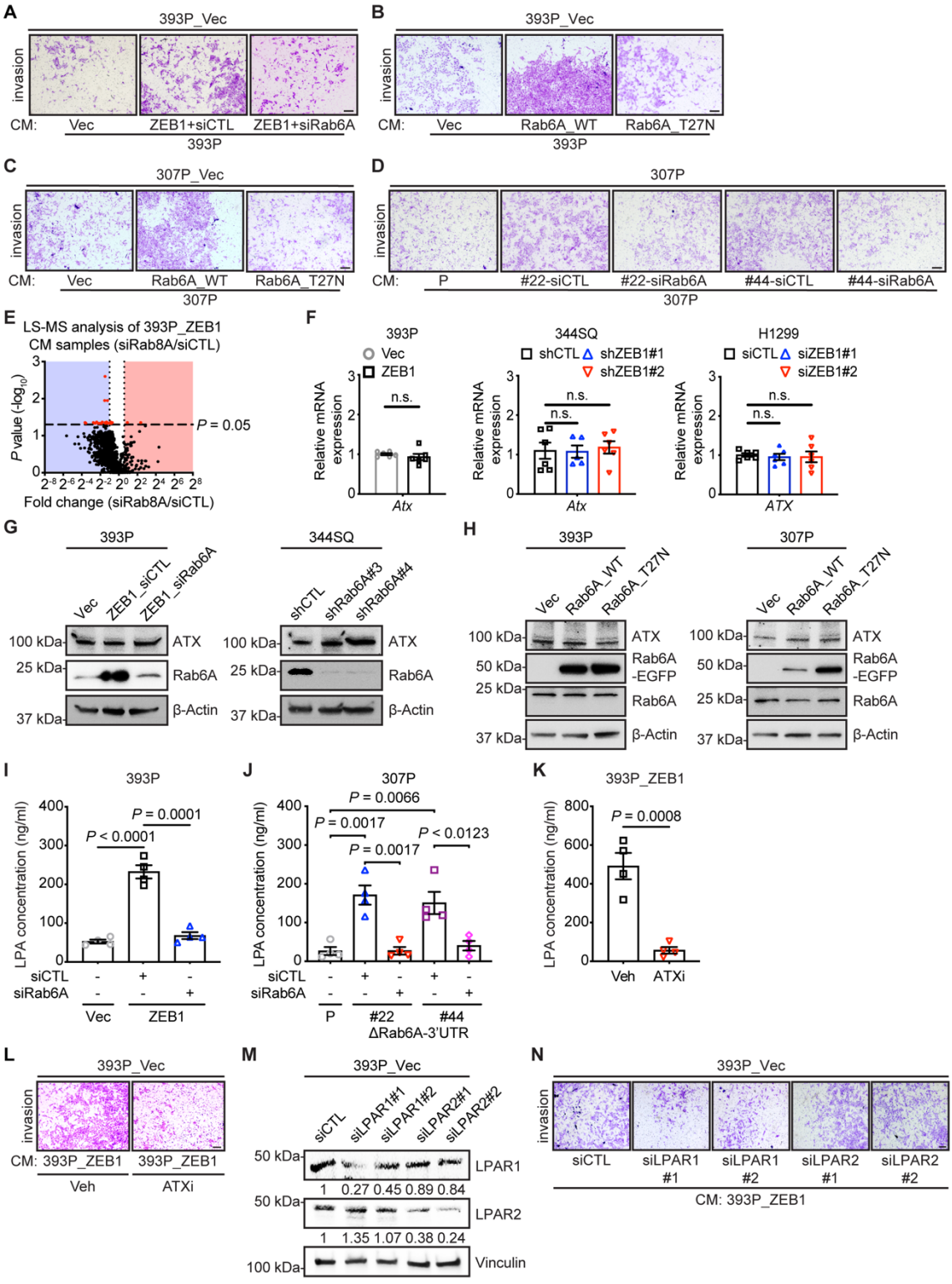
A
393P_Vec
invasion
CM: Vec ZEB1+siCTL ZEB1+siRab6A
393P
B
393P_Vec
invasion
CM: Vec Rab6A_WT Rab6A_T27N
393P
C
307P_Vec
invasion
CM: Vec Rab6A_WT Rab6A_T27N
307P
D
307P
invasion
CM: P #22-siCTL #22-siRab6A #44-siCTL #44-siRab6A
307P
E
LS-MS analysis of 393P_ZEB1
CM samples (siRab8A/siCTL)
P value (-log10)
P = 0.05
Fold change (siRab8A/siCTL)
F
393P
Vec
ZEB1
Relative mRNA expression
n.s.
Atx
344SQ
shCTL shZEB1#1
shZEB1#2
n.s.
Atx
H1299
siCTL siZEB1#1
siZEB1#2
n.s.
ATX
G
393P
Vec
ZEB1_siCTL
ZEB1_siRab6A
100 kDa ATX
25 kDa Rab6A
37 kDa β-Actin
344SQ
shCTL
shRab6A#3
shRab6A#4
100 kDa ATX
25 kDa Rab6A
37 kDa β-Actin
H
393P
Vec
Rab6A_WT
Rab6A_T27N
100 kDa ATX
50 kDa Rab6A -EGFP
25 kDa Rab6A
37 kDa β-Actin
307P
Vec
Rab6A_WT
Rab6A_T27N
100 kDa ATX
50 kDa Rab6A -EGFP
25 kDa Rab6A
37 kDa β-Actin
I
393P
LPA concentration (ng/ml)
P = 0.0001
P < 0.0001
siCTL
siRab6A
Vec
ZEB1
J
307P
LPA concentration (ng/ml)
P = 0.0066
P = 0.0017
P = 0.0017
P < 0.0123
siCTL
siRab6A
P
#22
#44
ΔRab6A-3'UTR
K
393P_ZEB1
LPA concentration (ng/ml)
P = 0.0008
Veh
ATXi
L
393P_Vec
invasion
CM: 393P_ZEB1 393P_ZEB1
Veh
ATXi
M
393P_Vec
siCTL
siLPAR1#1
siLPAR1#2
siLPAR2#1
siLPAR2#2
50 kDa LPAR1
1 0.27 0.45 0.89 0.84
50 kDa LPAR2
1 1.35 1.07 0.38 0.24
100 kDa Vinculin
N
393P_Vec
invasion
siCTL
siLPAR1 #1
siLPAR1 #2
siLPAR2 #1
siLPAR2 #2
CM: 393P_ZEB1

Fig. S5. The ZEB1/mR-148a/Rab6A axis promotes cancer cell invasion via a ATX/LPA-dependent pathway. (A-D) Bright field micrographs of cells that invaded through Matrigel-coated filters in Boyden chambers. Scale bar, 200 μm. Upper chambers contained CM from the indicated cells. (E) Volcano plot of proteins identified by LC-MS analysis of CM samples. *P* values (Y axis) and fold-change (X axis). Proteins at significantly different concentrations (red dots, $P < 0.05$) in Rab8A-deficient and -replete 393P_ZEB1 cells. (F) Q-PCR analysis of *ATX* mRNA levels in the indicated cells (n=6 replicates per condition). Control shRNA or siRNA sequences (CTL). (G) WB analysis shows that ATX levels in whole cell lysates are not altered by ectopic ZEB1 expression or Rab6A depletion. β-actin loading control. (H) WB analysis shows that ATX levels in whole cell lysates do not change following ectopic wild-type or enzyme-dead mutant Rab6A expression. (I-K) ELISA of LPA concentrations in CM samples from the indicated cells (n=4 replicates per condition). (L) Bright field micrographs of cells that invaded through Matrigel-coated filters in Boyden chambers. Scale bar, 200 μm. Upper chambers loaded with 393P_ZEB1 cell-derived CM and ATX inhibitor (ATXi) or vehicle. (M) WB analysis to confirm target gene depletion following transfection of LPAR1 or LPAR2 siRNAs. Relative densitometric values indicated. Vinculin loading control. (N) Bright field micrographs of siRNA-transfected 393P_vector cells that invaded through Matrigel-coated filters in Boyden chambers. Scale bar, 200 μm. Cells were transfected with LPAR1 or LPAR2 siRNAs. Upper chambers contained 393P_ZEB1 cell-derived CM.

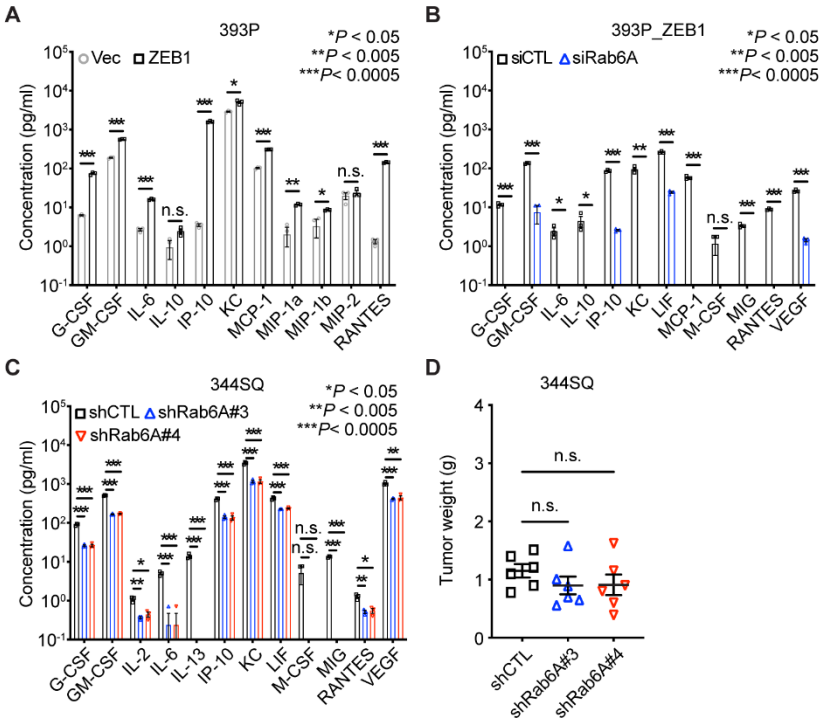

Fig. S6. ZEB1 activates a Rab6A-dependent secretory process. (A-C) Multiplexed antibody-based analysis of cytokine concentrations in CM samples from 393P_vector and 393P_ZEB1 cells (A), Rab6A-deficient or -replete 393P_ZEB1 cells (B), or Rab6A-deficient or -replete 344SQ cells (C) (n=triplicate samples per condition). (D) Flank tumor weights in syngeneic, immunocompetent mice (dots) 3 weeks after injection with Rab6A-deficient (shRab6A#3 and #4) or –replete (shCTL) 344SQ cells. Tumors analyzed by flow cytometric analysis (Fig. 4B).

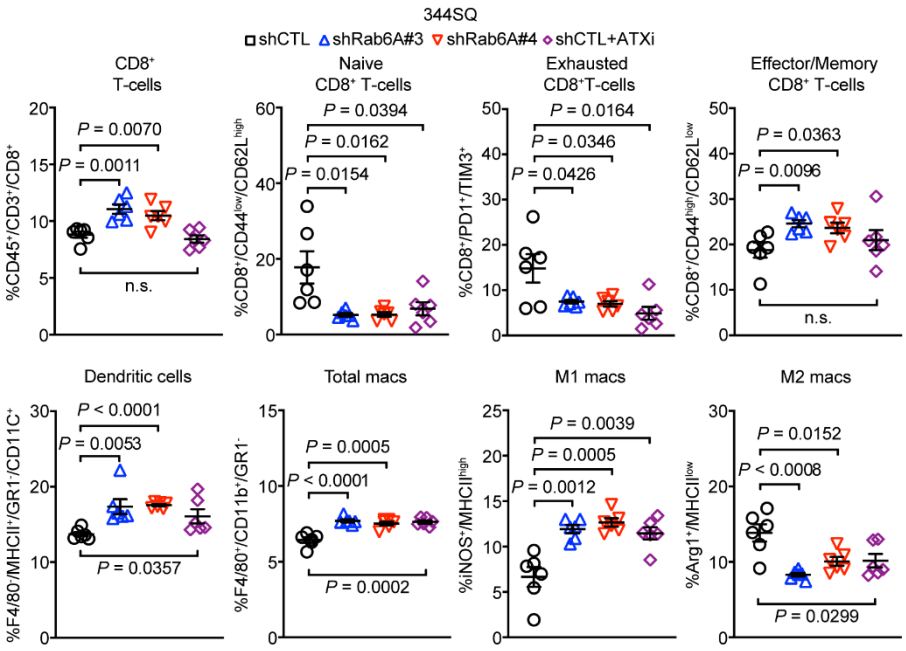

Fig. S7. ATX inhibition partly recapitulates the effects of Rab6A depletion on CD8+ T cells and macrophages. Flow cytometric analysis of murine splenocytes derived from syngeneic, immunocompetent mice that had been co-cultured with Rab6A-replete 344SQ cells in presence or absence of ATX inhibitor (n = 6 replicates of each condition). As a comparison, splenocytes were co-cultured with Rab6A-deficient 344SQ cells. Percentages of T cells (CD8+ T cells, CD44high/CD62Lhigh naïve CD8+ T cells, PD1+/TIM3+ exhausted CD8+ T cells, CD44high/CD62Llow effector/memory CD8+ T cells) and antigen-presenting cells (dendritic cells, total macrophages, M1 macrophages, and M2 macrophages) were quantified.

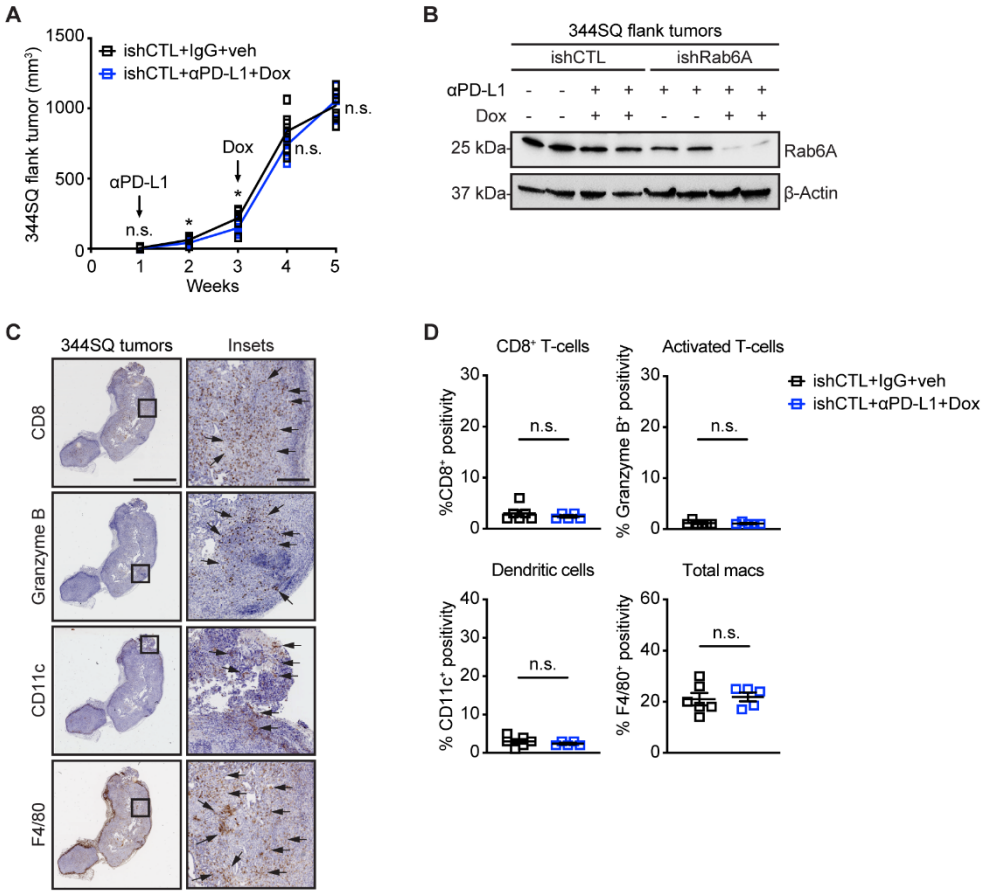

Fig. S8. LUAD cells acquire resistance to anti-PD-L1 treatment. (A) Subcutaneous tumor growth curves in syngeneic, immunocompetent mice (dots). Cohorts are color-coded. Mean ± SEM. ***, P < 0.0005. (B) WB analysis of Rab6A levels in flank tumors generated by 344SQ cells stably transfected with doxycycline (dox)-inducible control (ishCTL) or Rab6A (ishRab6A) shRNAs. Mice were treated with anti-PD-L1 (+) or IgG (-) and doxycycline (+) or vehicle (-). β-Actin loading control. (C) Representative images of tumor sections stained with anti-CD8, -granzyme B, -CD11c, or -F4/80 antibodies. Areas of interest (boxed regions) are illustrated at higher magnification (right column). Positively stained cells (arrows). Scale bars, 3 mm (left), 300 μm (insets). (D) The percentages of cells that stained positively in control (ishCTL+IgG+veh) and anti-PD-L1 (ishCTL+anti-PD-L1+Dox) cohorts.

Table S1. Characteristics of LUAD cell lines.

Cell line[a]	Species	ZEB1 expression	EMT state	Metastatic potential	References
307P	Mouse	Low	Epithelial	Low	(1)
393P	Mouse	Low	Epithelial	Low	(1)
393P_Vec[b]	Mouse	Low	Epithelial	Low	(2)
393P_ZEB1[c]	Mouse	High, ectopic	Mesenchymal	Medium	(2)
344SQ	Mouse	High	Mesenchymal	High	(1)
344SQ_shCTL[d]	Mouse	High	Mesenchymal	High	(2)
344SQ_shZEB1[e]	Mouse	Low, knockdown	Epithelial	Low	(2)
H1299	Human	High	Mesenchymal	High	(3)

[a]Murine cell lines designated based on mouse number (e.g., 307) and site of derivation, including primary lung tumor (P) or subcutaneous metastasis (SQ)

[b]stably transfected with empty vector

[c]stably transfected with ectopic ZEB1

[d]stably transfected with control shRNA

[e]stably transfected with ZEB1 shRNA

Table S2. Target Scan predicted miRNA binding sites.

miRNA	Position in the Rab6A 3'UTR	Seed match	Context++ score percentile
mmu-miR-148a-3p	534-540	7mer-1A	92
mmu-miR-182-3p	951-957	7mer-m8	89

miRNA	Position in the Rab6A 3'UTR	Seed match	Context++ score percentile
hsa-miR-148a-3p	571-577	7mer-1A	92

miRNA	Position in the Rab8A 3'UTR	Seed match	Context++ score percentile
mmu-miR-148a-3p	1193-1198	6mer	

miRNA	Position in the Rab8A 3'UTR	Seed match	Context++ score percentile
hsa-miR-148a-3p	1291-1296	6mer	

miRNA	Position in the Rgp1 3'UTR	Seed match	Context++ score percentile
mmu-miR-148a-5p	2951-2958	8mer	51
mmu-miR-182-3p	406-413	8mer	81
mmu-miR-182-5p	1708-1714	7mer-1A	13

miRNA	Position in the Rabin8 3'UTR	Seed match	Context++ score percentile
mmu-miR-148a-3p	614-620	7mer-1A	77

Table S3. List of qPCR primers.

Gene	Forward (5'-3')	Reverse (5'-3')
Mouse Rab1A	GTCCAGCATGAATCCCGAATA	ATCTGCAAACCTAAGGAGAAGG
Mouse Rab2A	GCAGGAGTCCTTTCGTTCTATC	GTTGAACGTGTCTCTCCTTGT
Mouse Rab5A	GGTCCCTTCATATGAGCTTCTT	CTGTTCCAGACACACCTCTATG
Mouse Rab6A	CTTCCCTGTTCTTCCCTTTCTC	TAGCCTGGAGCTGTCTGTAA
Human Rab6A	CACAGGACAGAAGCAGAGAAG	CATGGGAGATTAGCAGGAACAG
Mouse Rab7	CCTACTCAAAGAGGAAAGGAGAAC	GCTAACCTACAGGTACCACAAC
Mouse Rab8A	GCTCGATGGCAAGAGGATTA	CTGTAGTAGGCTGTCGTGATTG
Human Rab8A	CTGTACTCACAGCCAAGATCAC	GAGGATTCTGGATGCTTCTGTC
Mouse Rab11A	TGTAGAGCGATGGCTGAAAG	CTGCCCTGAGATGACGTAAAT
Mouse Rab14	AACTGCACCGTACAACTACTC	TGTGAGGACAATCAGCCATAAA
Mouse Rab23	TCTCGGCCTAAGAAGGAGATAG	GTCACCTTGAGTGGAGAAGAAA
Mouse Rab25	CCTGCCTTCAGCTTTCAGATA	GATCACATGGTAGGGCATGAT
Mouse Rab37	CAGAGGTCAGAGCCAGATAAAG	AAAGAGAGAGAGGGAGAGAGAG
Mouse Rab40B	CAAGCTCAAGGCCCATCTAA	GTCTGGAAAGGTCTCTGTCTTC
Mouse Rgp1	GAACTCACCCATCACCTTACTC	GTCCTTCTTCCCACTGTCATC
Human Rgp1	ATTGAGAGCATGGGCTGTAG	GGCTCAGAGAGGTGAAGTAATC
Mouse Rabin8	CTCCTTCCTGTCTGTGTGTATG	CGCGCACTGTTCTTCATTTATT
Human Rabin8	CAGGATGACGACTTGATGTAGAA	AGGGAGTAGGATCAGGAAGATAA
Mouse Mmp14	CATCATTGAGGTGGATGAGGAG	CCATGGCGTCTGAAGAAGAA
Human MMP14	GACTGTCAGGAATGAGGATCTG	CGTGTCCATCCACTGGTAAA
Mouse Atx	GTCCTCTCTCTGTGTCTTCTTTC	CATGAGTTCCTCTACCCACTTC
Human ATX	GGGCTGCACTTGTGATGATA	GAGGAGGTGTCTCTCTTCTGTA

References

1. D. L. Gibbons *et al.*, Contextual extracellular cues promote tumor cell EMT and metastasis by regulating miR-200 family expression. *Genes Dev* **23**, 2140-2151 (2009).
2. X. Tan *et al.*, Epithelial-to-mesenchymal transition drives a pro-metastatic Golgi compaction process through scaffolding protein PAQR11. *J Clin Invest* **127**, 117-131 (2017).
3. Y. H. Ahn *et al.*, ZEB1 drives prometastatic actin cytoskeletal remodeling by downregulating miR-34a expression. *J Clin Invest* **122**, 3170-3183 (2012).